SAND2000-2096J

Low-^{18}O Silicic Magmas: Why Are They So Rare?

Steven D. Balsley*
Robert T. Gregory

Stable Isotope Laboratory
Department of Geological Sciences
Southern Methodist University
Dallas, TX 75275-0395

* Now at:
Sandia National Laboratories
P. O. Box 5800
Albuquerque, NM 87185-0871 USA

Submitted to Earth and Planetary Science Letters

Abstract

Low-^{18}O silicic magmas are reported from only a small number of localities (e.g., Yellowstone and Iceland), yet petrologic evidence points to upper crustal assimilation coupled with fractional crystallization (AFC) during magma genesis for nearly all silicic magmas. The rarity of low-^{18}O magmas in intracontinental caldera settings is remarkable given the evidence of intense low-^{18}O meteoric hydrothermal alteration in the subvolcanic remnants of larger caldera systems. In the Platoro caldera complex, regional ignimbrites (150-1000 km^3) have plagioclase δ^{18}O values of 6.8 ± 0.1‰, whereas the Middle Tuff, a small-volume (est. 50-100 km^3) post-caldera collapse pyroclastic sequence, has plagioclase δ^{18}O values between 5.5 and 6.8‰. On average, the plagioclase phenocrysts from the Middle Tuff are depleted by only 0.3‰ relative to those in the regional tuffs. At Yellowstone, small-volume post-caldera collapse intracaldera rhyolites are up to 5.5‰ depleted relative to the regional ignimbrites. Two important differences between the Middle Tuff and the Yellowstone low-^{18}O rhyolites elucidate the problem. Middle Tuff magmas reached water saturation and erupted explosively, whereas most of the low-^{18}O Yellowstone rhyolites erupted effusively as domes or flows, and are nearly devoid of hydrous phenocrysts. Comparing the two eruptive types indicates that assimilation of low-^{18}O material, combined with fractional crystallization, drives silicic melts to water oversaturation. Water saturated magmas either erupt explosively or quench as subsurface porphyries *before* the magmatic ^{18}O can be dramatically lowered. Partial melting of low-^{18}O subvolcanic rocks by near-anhydrous magmas at Yellowstone produced small-volume, low-^{18}O magmas directly, thereby circumventing the water saturation barrier encountered through normal AFC processes.

Introduction

The rarity of erupted, low-^{18}O magmas in intracontinental settings is puzzling given: (1) the evidence of intense, low-^{18}O meteoric/hydrothermal alteration in the subvolcanic remnants of large caldera systems [1-4], and (2) petrologic evidence that points to upper crustal assimilation coupled with fractional crystallization (AFC) during differentiation for nearly all silicic magmas [5-9]. Volcanic fields where calderas are developed are among the most geothermally active regions on earth, and sustain meteoric hydrothermal systems of great size (altered host rock volumes up to 10^3 km^3 and integrated fluid-rock ratios ~~of~~ on the order of 1) for geologically significant time periods (10^5 -10^6 y) [10]. The depth to which hydrothermal alteration may extend in these environments may reach 3-5 km [11], well within the range of magma chamber depths.

Despite persistent efforts, to date only a handful of locations are known in which unambiguously low-^{18}O magmas have erupted: Iceland [12, 13], Oasis Valley-Timber Mountain caldera complex, Nevada [14], the Yellowstone Plateau volcanic field, Wyoming [15, 16], and the Calabozos caldera complex [17].

Larson and Taylor [18, see also 19] measured oxygen isotope ratios of phenocrysts from ignimbrites of the central Nevada and San Juan caldera complexes in an attempt to demonstrate the link between caldera-related volcanic systems and the formation of low-^{18}O rhyolitic magmas, but did not observe the spectacular types of low-^{18}O magmas observed at Yellowstone by Hildreth et al. [16]. Larson and Taylor [18] tentatively concluded that the rarity of low-^{18}O rhyolitic magmas was linked to an indeterminate combination of factors such as the duration of magmatism, the extent of hydrothermal alteration, and the magnitude of extensional tectonic activity. Here we shed further light on this problem by considering petrologic, isotopic and volcanologic data from two multicyclic caldera centers: the Yellowstone Plateau volcanic field, Wyoming

[16], and Platoro caldera complex of the southeast San Juan volcanic field, Colorado [20] (fig. 1).

At Yellowstone, Hildreth et al. [16] reported ^{18}O depletions up to 5.5 per mil (‰) from unaltered intracaldera rhyolite lavas that erupted following two separate cycles of caldera collapse; these are among the lowest known primary $\delta^{18}O$ values from rhyolitic magmas. Two aspects of ^{18}O-depleted rhyolites from Yellowstone are noteworthy: (1) with few exceptions, all were erupted as either domes or lavas, and (2) the phenocryst assemblage lacks hydrous phases.

Evidence of ^{18}O depletion is conspicuously less pronounced (<0.5‰) among pyroclastic deposits associated with early post-collapse cycles of the Platoro caldera complex [21]. Post-caldera collapse rocks at Platoro were produced by a series of pyroclastic eruptions and contain abundant biotite and/or hornblende phenocrysts. Given the fact that abundant low-^{18}O crustal material was available in the sub-volcanic realm of both fields, we propose that the solubility of water in high-silica magmas and its profound effect on the solidus are key to understanding why low-^{18}O magmas are rare. Furthermore, when the effects of water solubility on the efficacy of AFC are factored into the eruptive history of caldera complexes, slight ^{18}O depletions such as observed at the Platoro caldera complex may be more common than previously thought.

Sample Preparation and Analytical Methods

Forty-seven new $\delta^{18}O$ values were measured from andesites to dacites of the Platoro caldera complex. None of these rocks contain quartz, therefore it was necessary to focus primarily on plagioclase phenocrysts, which occur in all of the units of interest. Most plagioclase crystals were extracted from non-welded to welded pumice clasts. To avoid secondary effects in glassy pumice clasts, samples were collected from rapidly cooled airfall deposits and flow units located 10-15 km from the rim of the Platoro caldera, well away from any known zones of hydrothermal alteration. In addition to plagioclase, oxygen isotope ratios were measured on biotite, augite and hornblende phenocrysts. All mineral separates were inspected under binocular microscopes and hand picked to ensure high purity.

Oxygen was extracted using a ClF_3 procedure similar to that described by Taylor and Epstein [22] and Borthwick and Harmon [23], and converted to CO_2 by reaction with heated graphite for mass spectrometric analysis. The small differences among Middle Tuff and regional ignimbrite samples required repetitious analyses of standards and unknowns. Inter-run variability was monitored with a well characterized internal laboratory quartz standard, which routinely had a reproducibility of ± 0.1‰, as well as by multiple analyses of unknowns. Repeat analyses of plagioclase samples yielded $\delta^{18}O$ standard deviations no greater than 0.3‰, excluding two samples (SB-96 and MD-43; see Tables 2 and 3) with standard deviations of ~0.5 ‰. These samples also have elevated trace element concentrations compared to other dacites, indicating a derivation from a common magma with xenocrystic plagioclase. The average standard deviation on the remaining 22 samples for which multiple analyses were performed is 0.1‰. Oxygen isotopic data from Yellowstone rhyolites are taken from Hildreth et al. [16], and reference to the analytical procedures used may be found therein.

Two Caldera Systems: The ^{18}O Perspective

Platoro Caldera Complex

The Platoro caldera complex (fig. 1), located in the southeast San Juan volcanic field, Colorado, was originally described by Lipman et al. [24] and Lipman [14] as a nested caldera structure, inferring at least a dual collapse history. Recent stratigraphic revisions [25], prompted by high-precision age determinations, new field interpretations and mineral chemical and paleomagnetic data, reveal at least six caldera subsidence events within the Platoro complex. The bulk of the pyroclastic geology of the southeast San Juans occurs within the Treasure Mountain Group [25], which is composed of eight pyroclastic rock units. The ~29.5 Ma Middle Tuff is a moderate volume (est. 50-100 km^3), post-caldera collapse sequence composed of at least 9 minor-volume, coupled pyroclastic fall and flow deposits. The Middle Tuff lies stratigraphically above the La Jara Canyon Tuff (est. 1000 km^3) and rests beneath the Ojito Creek (est. 100 km^3) and Ra Jadero (est. 50 km^3) tuffs. There is a possibility that the Middle Tuff eruption may have been large enough to cause caldera subsidence [25].

Evidence of extensive hydrothermal circulation in the Platoro caldera complex occurs in and around several intracaldera intrusive bodies ranging in age from ~29 to ~23 Ma [24, 26]. Hydrothermal alteration was likely associated with intrusion of intermediate-composition magmas into the sub-volcanic crust following caldera-related subsidence. A close association among zones of intense hydrothermal alteration and fault intersections is evident throughout the Platoro caldera complex. Mineralization associated with alteration in the eastern caldera region resulted in quartz-pyrite veins from which small amounts of rich gold-silver ore were produced. The most significant gold-bearing ores occur near the northwest rim of the Platoro caldera in the Summitville district, where quartz-alunite-pyrite replacement of silicic dacites is interpreted to be the result of shallow solfataric activity [27]. The geology and geochemistry of the Summitville Mining District indicate a strong association with magmatism [14, 26].

Large variations in phenocryst content are apparent among andesite to silicic dacite pumice in the Middle Tuff (fig. 2). Open-system magmatic processes (magma mixing, assimilation combined with fractional crystallization) are invoked for most of the observed petrographic, mineral chemical, and whole-rock geochemical discontinuities in the Middle Tuff [21]. In general, Middle Tuff samples are similar in whole-rock and mineral composition to the La Jara Canyon, Ojito Creek and Ra Jadero tuffs. The gross similarity in major element composition among Treasure Mountain Group rocks indicates that these magmas erupted at or near cotectic conditions, so that the major element chemistry was essentially buffered by the fractionating mineral assemblages. Incompatible trace elements also cluster at similar concentrations among most Treasure Mountain Group rocks.

Colucci et al. [28] found that the evolved character of pre-caldera intermediate-composition rocks formed a substantial impediment to evaluating the processes that affected early magmas, and therefore, in determining the compositions of primary mantle-derived liquids beneath the southeast San Juans. Even the most primitive pre-caldera rocks that might be considered parental are only marginally basaltic (<5% MgO, <90 ppm Ni) and are highly evolved relative to liquids that might be in equilibrium with normal mantle compositions (>10% MgO, >300 ppm Ni). In order to derive these parental melts from primary mantle magma, significant crystal fractionation is required, and/or significant quantities of crust must be added to modify the composition of either the mantle source or the primary melts.

Sr, Nd and Pb isotopic studies [28, 29] indicate that all intermediate-composition rocks and silicic pyroclastic rocks in the Platoro complex all underwent some degree of crustal contamination. Sr isotopes are remarkably homogeneous among Treasure Mountain magmas (average 0.7051) including the Middle Tuff, which precludes significant involvement of "typical" radiogenic Proterozoic basement [e.g., 30], and allows a significant contribution from low, time-integrated Rb/Sr lower crust, or anomalously ^{87}Rb enriched upper mantle. Nd isotopes are too heterogeneous (variation up to 8 ε_{Nd} units; Balsley, unpublished data) to have originated from a single homogenous mantle source. Pb isotopes are remarkably uniform across the range of Middle Tuff compositions and overlap with relatively non-radiogenic intermediate-composition andesites. These are interpreted as lower crustal signatures [28, 29]. Because it is likely that all parental andesite magmas underwent substantial crustal contamination, it is probable that later differentiates were subject to additional shallow level contamination.

Petrography

Plagioclase is the most abundant phenocryst in the Middle Tuff (fig. 2) and the $\delta^{18}O$ range of 38 samples is about 1.3‰, from 5.5 to 6.8 (table 2), although only three samples define the lower end of the range. The average $\delta^{18}O$ value of the remaining 35 samples is 6.5 ± 0.2‰. Biotite, augite and hornblende phenocrysts show more erratic variations in $\delta^{18}O$ values than plagioclase, which may be caused by microphenocryst inclusions, xenocrystic contamination or small amounts of secondary alteration along cleavage fractures. Mineral disequilibrium is also indicated by negative values of $\Delta^{18}O_{plag\text{-}biotite}$, $\Delta^{18}O_{plag\text{-}augite}$ and $\Delta^{18}O_{plag\text{-}hornblende}$ (fig. 3). Crystallization of co-magmatic minerals should never produce negative fractionations (Δ) between plagioclase and augite. Mixing of magmas of different oxygen isotope composition can produce phenocryst pairs with reversed fractionations. $\delta^{18}O$ estimates for the various whole-rock values of magma types were therefore not considered because of evidence for mineral disequilibrium and the fact that feldspars furnish a reasonable estimate of the magmatic ^{18}O value and, because at silicic magma temperatures, $\delta^{18}O$ magma-feldspar fractionations are 0.2 to 0.3‰ [31]. No noticeable variation in $\delta^{18}O$ is observed with increasing SiO_2, and no correlation between $\delta^{18}O$ and magma type is evident among any Middle Tuff samples.

Open-system magmatic processes are evident in the petrography of andesitic to silicic dacitic pumices throughout the Middle Tuff sequence: (1) mineral zoning (normal and reversed), (2) embayed and resorbed grains, (3) overgrowths of younger liquidus phases over older liquidus phases, and (4) multiple populations of the same liquidus phases with distinctive compositions in the same pumice. These textural data indicate incomplete mixing of different composition magmas and possibly incomplete assimilation.

Regional ignimbrites of the Treasure Mountain Group exhibit comparatively uniform plagioclase $\delta^{18}O$ compositions (mean 6.8 ± 0.1‰ table 3), but show nonequilibrium fractionations between plagioclase and mafic phenocrysts (fig. 3), similar to those observed in the Middle Tuff. Many of the same open system petrographic features in the Middle Tuff are also found in the regional units. Significantly, the relatively small-volume pyroclastic units of the Middle Tuff have mean plagioclase $\delta^{18}O$ values about 0.3‰ below that of the mean value from the surrounding regional ignimbrites, irrespective of composition and age (fig. 4). None of the 38 samples show the depleted $\delta^{18}O$ values recognized at Yellowstone, in spite of the apparently favorable conditions for interaction of Middle Tuff magmas with ^{18}O depleted rocks and/or fluids. Nevertheless these data indicate a small (~0.3‰) but significant lowering of the $\delta^{18}O$ values of Middle Tuff magmas with respect to the larger-volume, ^{18}O-homogeneous regional ignimbrite magmas.

Low ^{18}O Yellowstone Rhyolites

The 17,000 km^2 Yellowstone volcanic field underwent three cycles of caldera-forming activity at 2.0, 1.3 and 0.64 Ma, producing the Huckleberry Ridge Tuff (HRT: 2500 km^3), Mesa Falls Tuff (MFT: 280 km^3) and Lava Creek Tuff (LCT: 1000 km^3), respectively [32]. The following discussion of oxygen isotope data from Yellowstone is based on two papers by Hildreth and co-workers [16, 33]: (1) a comprehensive $\delta^{18}O$ study of more than 150 rhyolitic ignimbrites, lavas and domes associated with and postdating caldera formation, as well as 30 different basalt samples [16], and (2) a chemical and radioisotopic study of the basalts and rhyolites of the Yellowstone Plateau [33]. The three regional ignimbrites at Yellowstone have quartz $\delta^{18}O$ values between 7.3 and 5.6‰ (table 3, fig. 5), corresponding to magmatic $\delta^{18}O$ values of 6.9 to 4.8‰. There is no overlap in quartz δ^{18}O values among the regional ignimbrites, and the quartz δ^{18}O values within each unit is narrow (0.3-0.7‰) despite significant whole-pumice compositional zonation. Taylor's [4, 31] compilation of δ^{18}O values from igneous rocks constrains most silicic volcanic rocks to between 7 and 10‰, suggesting that the Yellowstone ignimbrites are slightly to moderately depleted in ^{18}O relative to "average" values.

In contrast to the relatively small range in quartz δ^{18}O values among the regional ignimbrites, post-caldera collapse intracaldera rhyolites exhibit exceptionally large ^{18}O depletions (table 3, fig. 5). Post-caldera collapse rhyolites associated with the first and third cycle rhyolites are depleted 3.3 to 5.5‰ relative to the HRT and LCT, respectively; a comparatively small depletion in ^{18}O (~0.3‰) is observed in post-caldera collapse rocks associated with the second caldera cycle. Radiometric age determinations (K-Ar) of sanidine phenocrysts reveal that the period between caldera formation and eruption of the low-^{18}O rhyolites was as short as 0.05 to 0.1 million years. Significantly, the interval during which ^{18}O depletion occurred (the repose time between collapse events) was also geologically brief, lasting between 0.3 and 0.5 million years. A summary of the salient petrographic and petrologic features of low-^{18}O Yellowstone rhyolites is presented below.

Petrography

Two rhyolite flows with a combined volume of 10-20 km^3 are associated with the first caldera cycle. The Blue Creek and Headquarters flows both contain 15-20% phenocrysts of quartz, sanidine, plagioclase, clinopyroxene, fayalite, and Fe-Ti oxides. Xenocrysts/xenolithic fragments are absent from all samples. Both flows are compositionally similar to the underlying HRT and are interpreted to be late-erupted extracts from the HRT magma chamber that survived collapse.

Post-caldera collapse rhyolites associated with the second cycle are preserved as a series of five domes that collectively have a volume of 1-2 km^3, although many more times this volume is probably buried beneath younger units. All samples contain large phenocrysts of quartz and feldspar, with the total phenocryst abundance between 25 and 40%. No xenocrystic or xenolithic fragments are present.

The third cycle consists of rocks with the most depleted $\delta^{18}O$ values recognized at Yellowstone. Low-^{18}O rhyolites associated with the youngest caldera cycle erupted along two separate regions of the caldera ring fracture. The first group of flows includes the Tuff of Uncle Tom's Cabin, the Tuff of Sulfur Creek and the Canyon Flow lava, which collectively represent 40-70 km^3 of magma. The second group of ^{18}O depleted rhyolites consists of the Biscuit Basin Flow, which has a volume of 2.5 to 25 km^3 and a phenocryst assemblage including quartz, feldspar and Fe-Ti oxides.

Extracaldera rhyolites that erupted contemporaneously with low-^{18}O intracaldera units show no appreciable drop in $\delta^{18}O$ values compared to the regional ignimbrites, indicating that ^{18}O depleted rhyolite magmas were stored in sub-caldera chambers. Significantly, none of the ^{18}O depleted post-caldera collapse lavas of the first and third cycles at Yellowstone contains hydrous phenocrysts.

Hildreth et al. [16] also observed no petrographic evidence for assimilation of hydrothermally altered country rocks in any of the low-^{18}O rhyolite samples. Significantly, near-uninterrupted trace element trends from the LCT through low-^{18}O rhyolites erupted during the early stage of the third caldera cycle strongly suggest a common magma reservoir for these rhyolites. Fe-Ti oxide temperatures from the LCT (890°-900°C) are also indistinguishable from the later Biscuit Basin flow (~900°C). Temperatures calculated with isotope geothermometry using quartz-sanidine and quartz-magnetite pairs generally were higher than the Fe-Ti oxide temperatures (LCT: 890-1040°C; Biscuit Basin flow: 1040°C), and may not be reliable due to poor temperature concordancy between mineral pairs.

In comparing these two silicic caldera systems, the most striking difference (excluding their oxygen isotope values) are the eruptive styles of post-caldera collapse magmas (ignimbrites at Platoro and lavas at Yellowstone) and inferred water content for post-caldera collapse magmas (high at Platoro and low at Yellowstone). Interestingly, the magmas with the lowest water contents show the greatest ^{18}O depletions, whereas magmas that clearly reached water saturation show only minor ^{18}O depletion. This indicates a correlation between magmatic water content and the potential for lowering of ^{18}O in silicic magmatic systems.

Discussion

Mechanisms for producing low-^{18}O magmas have been discussed extensively [13, 16, 18, 34-36]. Hildreth et al. [16] called upon direct influx of low-^{18}O meteoric water into rhyolitic magma to explain the dramatic ^{18}O depletions at Yellowstone. Lipman and Friedman [14] also preferred a direct influx mechanism to explain depleted ^{18}O silicic melts in southwestern Nevada. On physical grounds, this mechanism is hampered because magmas sit at lithostatic pressure, whereas meteoric fluids lie on hydrostatic pressure gradients. Given the large pressure differential between the magmatic system and hydrothermal system, direct diffusion across the boundary layer is extremely difficult [19, 35, 37].

Taylor [19] pointed out that partial melting of hydrothermally altered wallrocks, and/or stoping of the same material, into the roof of a magma chamber more easily facilitates incorporation of low-^{18}O material. In a later paper, Hildreth et al. [33] used radiogenic isotopes to demonstrate that major contamination occurred at Yellowstone in association with the cycles of caldera collapse and resurgence, whereby large-scale assimilation of deeply buried volcanic rocks and their affiliated hydrothermal systems (rocks + fluids) must have occurred. Under these conditions, it is conceivable that low-

^{18}O contaminants, introduced incrementally over the 10^4 -10^5 y repose period between caldera subsidence events, would significantly alter the mean magmatic $\delta^{18}O$ value. Such a mechanism should by no means be considered unique to Yellowstone. Therefore the answer to what makes Yellowstone so unusual lies elsewhere.

In comparing the low-^{18}O signatures of the Middle Tuff to the regional Treasure Mountain Group ignimbrites, the important questions are: (1) why are the smaller-volume Middle Tuff units slightly depleted relative to the regional units, and (2) why are the depletions so much smaller than those observed at Yellowstone (i.e. caldera cycles 1 and 2)? If all related magmas in the Platoro caldera complex formed by similar processes, but differ only in their oxygen isotope compositions, then a more likely explanation relates the efficiency of assimilation (i.e. the uptake of low-^{18}O material) to the size and shape of smaller magma reservoirs such as the Middle Tuff. An important consequence of the volume difference is that effective surface area is inversely proportional to the size of a magma chamber.

Small Magma Chambers

Taylor [5] used material balance relationships to assess effects of wallrock assimilation/exchange on magmatic $\delta^{18}O$ values. For relatively simple cases, where $\Delta^{18}O_{c\text{-}m}$ ($\delta^{18}O_{cumulates}$ - $\delta^{18}O_{melt}$) approaches zero, the magmatic $\delta^{18}O$ value varies as a function of a modified Rayleigh law. In the AFC material balance equation, the important exponential variable is R, the ratio of cumulates to assimilated wallrock. As R decreases, the degree to which the magmatic $\delta^{18}O$ value is modified by crystallization becomes more significant at even small additional amounts of crystallization (fig 6). Small-volume magma chambers, with their larger surface area to volume ratios, may have lower values of R (even if it is for a short time), so that their $\delta^{18}O$ values evolve more rapidly as a function of crystallization (see slopes on fig 6). Just 10-20% additional crystallization of the small-volume melt in the presence of low-^{18}O wallrocks lowers the magmatic $\delta^{18}O$ value by a few tenths of a per mil.

The second important question regarding the ^{18}O lowering of Middle Tuff magmas is why the effect was not as pronounced as that observed in post-caldera collapse rhyolites at Yellowstone. Significantly, ^{18}O depleted post-caldera collapse rhyolites at Yellowstone erupted effusively, contain no hydrous phenocrysts, and generally have low whole-rock H_2O contents (table 3). Whole-rock H_2O values are notoriously unreliable gauges of magmatic water content because volcanic glasses are known to rapidly hydrate [38-42]. However, even if the Yellowstone samples are hydrated to some degree, the initial water content of the glasses must have been quite low because post-hydration H_2O contents are still generally 2 wt.%. That these magmas had low initial water contents is also supported by, (1) non-hydrated rhyolitic Yellowstone glasses that have reported water contents of 0.2-0.4 wt.% [43-45], and (2) $\Delta^{18}O_{quartz\text{-}glass}$ values of 0.5 and 0.3 ‰ for the Biscuit Basin Flow and Blue Creek Flow samples, respectively [16], suggesting that glasses from these two samples sustained little to no oxygen exchange with meteoric waters (present-day $\delta^{18}O$: -18‰). We nevertheless assume that Yellowstone whole-rock H_2O values represent crystallization-induced volatile loss at water saturation ($P_{H2O} = P_{Total}$), and therefore are low-end estimates of the pre-eruptive magmatic water content.

most dome
rhyolite flows
have H_2O <
0.2 wt%
⇒ eruption
mechanism

Low $\delta^{18}O$ Yellowstone rhyolites therefore probably formed as either direct partial melts of shallow level ^{18}O-depleted roof rocks, or they started out as dry, superheated magmas and were thus able to assimilate a much higher proportion of depleted wallrock and fluids before erupting. Geophysical evidence indicates that the present upper surface of magma at Yellowstone lies at depths between 6 and 10 km [46-48], corresponding to pressures between 2 and 3 kb. Maximum water solubilities in pegmatitic melts at these pressures range from about 6 to 8 weight percent [49], which is a reasonable analogue for rhyolite magmas at Yellowstone. Using these general parameters as guidelines, water-poor Yellowstone magmas would have an enhanced capacity to assimilate or partially melt water-rich crustal material before reaching water saturation.

Effect of Water Saturation on AFC

In contrast to low-^{18}O Yellowstone rhyolites, Middle Tuff dacitic magmas erupted explosively and contain abundant hydrous phenocrysts; at least 4-5 wt.% H_2O is necessary for hornblende crystallization [50], which is present in many units. That Middle Tuff magmas were at or near water saturation is implicit from the hydrous phase mineralogy and explosive eruptive style. Rhyolitic magmas usually contain at least ~4-6 wt % H_2O prior to eruption [51-54], and for silicic magma systems studied in detail volatile saturation prior to eruption is considered probable [55]. For magmas under conditions of $P_{H2O} < P_{Total}$, melting curves assume positive slopes in P-T space.

However, for water-saturated conditions the melting curve acquires a negative Clapeyron slope. The greatest effect of water saturation on an ascending magma is to effectively quench the system, resulting in the formation of a porphyritic intrusion, or if the volume change of H_2O is large enough and occurs at shallow crustal depths the system may erupt.

The major element compositions of magmas from both fields were controlled by cotectic or near-cotectic crystallization trajectories. Once *any* magma reaches a cotectic the major element composition of fractionated liquids will be little changed by AFC because the position of the cotectics, and not the contaminant, controls the major element composition. However the trace elements, and particularly the isotopic ratios, will likely be modified by open-system processes [5, 56].

Water Saturation Barrier for AFC

In figure 7 the combined affects of limited crystallization and magmatic water content are shown for a silicic magma undergoing AFC. The mineral/liquid distribution coefficient for water is small for most hydrous magmas ($\beta = 0.2$). The ratio of cumulates to assimilant (R) is usually >>1, probably in the range 5-10, due to the energetics of partial melting; a value of 5 is used for this example, meaning that for every gram of assimilated material, 5g of cumulus minerals form on an oxygen basis. The calculations assume that magmatic $\delta^{18}O$ values are smoothly integrated across the chamber. For the model calculations, $\delta^{18}O$ for the starting magma and assimilant are set at 7 and -11‰, respectively. Also shown is the water saturation index as a function of fraction crystallized. For example a WSI of 1.2 implies the magma is 20% oversaturated in water. Three magmas with initial water saturation indices 0.5 - 0.75 - 0.85 increase their water content and hence saturation indices as crystallization proceeds. In the case of the least water-rich magma (WSI = 0.5), crystallization up to 50% (most silicic magmas erupt with <40% phenocrysts [57]) produces a ~3‰ drop in magmatic $\delta^{18}O$ values, whereas, for more realistically modeled magmas ($WSI_0 = 0.75$) assimilation produces a drop in just over 1‰.

The limit imposed on crystallization by water saturation in a dynamic system is what we refer to as a "water saturation barrier." Once this threshold is reached any further temperature and/or pressure drop must result in either quenching of the magma or violent eruption. A compilation of phenocryst abundances in silicic volcanic rocks with $SiO_2 > 60\%$ [57] shows that most magmas erupt well before reaching 30% crystallization. Clearly, many magmas reach water saturation before 20% crystallization, and thus the potential for ^{18}O lowering is limited in natural systems.

Conclusions

Magmatic water is the key to understanding why low-^{18}O magmas are rare. Water saturated magmas either erupt explosively or quench as subsurface porphyries before the magmatic ^{18}O can be dramatically lowered by AFC. Crystallization of the magma supplies the heat required to drive AFC and moves the magma to water saturation. Water saturation effectively acts as a barrier to further AFC because of the negative P-T slope of the water saturated melting curve. Any additional AFC beyond water saturation produces a vapor phase with a large volume change, which initiates an eruptive event at shallow depths. At greater depths, this process generates sub-caldera porphyry plutonic systems.

The post-caldera collapse magmas at Platoro are hydrous and erupted explosively, whereas at Yellowstone post-caldera collapse magmas have anhydrous phenocryst assemblages and erupted effusively as lavas. In a post-caldera collapse environment, more efficient AFC involving hydrous wallrocks quickly drives the residual magmas to water saturation triggering further explosive eruptions. Our Middle Tuff data indicate this occurs after small amounts of additional crystallization. This probably represents the most common scenario.

In contrast, low-^{18}O magmas at Yellowstone probably represent direct partial melts of sub-volcanic low-^{18}O rocks. This mechanism for Yellowstone clearly avoids the water saturation barrier that limits ^{18}O lowering by AFC. This also addresses the paradox of a low ^{18}O magma with only 15-20% phenocrysts. At this stage of crystallization, these magmas could only be lowered by 2‰ (see figure 7).

The small (0.3‰) depletion detected among Middle Tuff samples relative to the regional ignimbrites represents a smaller degree of ^{18}O lowering, consistent with the limitations imposed by the water saturation barrier. These effects are typically of order per mil or less. Without a detailed knowledge of the eruptive stratigraphy, these effects can be commonly overlooked.

Acknowledgments

John Wolff is thanked for helpful discussions and an early review of the manuscript. Kurt Ferguson provided useful The comments of three anonymous reviewers clarified a number of ideas. Sandia is a multiprogram laboratory operated by Sandia Corporation, a Lockheed Martin Company, for the United States Department of Energy under contract DE-AC04-94AL85000.

References

1 P.M. Bethke and R.O. Rye, Environment of ore deposition in the Creede mining district, San Juan Mountains, Colorado: Part IV. Sources of fluids from oxygen, hydrogen and carbon isotope studies, Econ. Geol. 74, 1832-1840, 1979.

2 J.R. O'Neil, M.L. Silberman, B.P. Fabbi and C.W. Chesterman, Stable isotope relations during mineralization in the Bodie mining district, Mono County, California, Econ. Geology 68, 765-784, 1973.

3 S.M.F. Sheppard and H.P. Taylor, Jr., Hydrogen and oxygen isotope evidence for the origins of water in the Butte ore deposits, Montana, Econ. Geol. 69, 926-946, 1974.

4 H.P. Taylor, Jr., The application of oxygen and hydrogen isotope studies to problems of hydrothermal alteration and ore deposits, Econ. Geol. 69, 843-883, 1974.

5 H.P. Taylor, Jr., The effects of assimilation of country rocks by magmas on $^{18}O/^{16}O$ and $^{87}Sr/^{86}Sr$ systematics in igneous rocks, Earth Planet. Sci. Lett. 47, 243-254, 1980.

6 P.W. Lipman, Evolution of silicic magma in the upper crust: the mid-Tertiary Latir volcanic field and its orogenic granitic batholith, northern New Mexico, USA, Trans. R. Soc. Edinburgh 79, 265-288, 1988.

7 C.R. Bacon, L.H. Adami and M.A. Lanphere, Direct evidence for the origin of low-^{18}O silicic magmas: quenched samples of a magma chamber's partially-fused granitoid walls, Crater Lake, Oregon, Earth Planet. Sci. Lett. 96, 199-208, 1989.

8 C.M. Johnson, Large-scale crust formation and lithospheric modification beneath middle to late Cenozoic calderas and volcanic fields, western North America, J. Geophys. Res. 96, 12,485-13,507, 1991.

9 L.R. Riciputi, C.M. Johnson, D.A. Sawyer and P.W. Lipman, Crustal and magmatic evolution in a large multicyclic caldera complex: isotopic evidence from the central San Juan volcanic field, J. Volcanol. Geotherm. Res. 67, 1-28, 1995.

10 R.E. Criss and H.P. Taylor, Jr., Meteoric-hydrothermal systems, in: Stable Isotopes in High Temperature Geologic Processes, H.P.T. J.W. Valley, Jr., J.R. O'Neil, ed., Rev. in Mineral. 16, pp. 373-422, Mineral. Soc. Amer., Chelsea, MI, 1986.

11 R.E. Criss and H.P. Taylor, Jr., An $^{18}O/^{16}O$ and D/H study of Tertiary hydrothermal systems in the southern half of Idaho, Geol. Soc. Amer. Bull. 94, 640-663, 1983.

12 K. Hattori and K. Muehlenbachs, Oxygen isotope ratios of the Icelandic crust, J. Geophys. Res. 87, 6559-6565, 1982.

13 K. Muehlenbachs, A.T. Anderson and G.E. Sigvaldsson, Low-^{18}O basalts from Iceland, Geochim. Cosmochim. Acta 38, 577-588, 1974.

14 P.W. Lipman and I. Friedman, Interaction of meteoric water with magma: an oxygen-isotope study of ash-flow sheets from southern Nevada, Geol. Soc. Amer. Bull., 695-702, 1975.

15 I. Friedman, P.W. Lipman, J.D. Obradovich, J.D. Gleason and R.L. Christiansen, Meteoric water in magmas, Science 184, 1069-1072, 1974.

16 W. Hildreth, R.L. Christiansen and J.R. O'Neil, Catastrophic isotopic modification of rhyolitic magma at times of caldera subsidence, Yellowstone Plateau volcanic field, J. Geophys. Res. 89, 8339-8369, 1984.

17 A.L. Grunder, Low $\delta^{18}O$ silicic volcanic rocks at the Calabozos caldera complex, southern Andes- evidence for upper crustal contamination, Contrib. Mineral. Petrol. 95, 71-81, 1987.

18 P.B. Larson and H.P. Taylor, Jr., $^{18}O/^{16}O$ ratios in ash-flow tuffs and lavas erupted from the central Nevada caldera complex and the central San Juan caldera complex, Colorado, Contrib Mineral Petrol 92, 146-156, 1986.

19 H.P. Taylor, Jr., Igneous rocks: I. Processes of isotopic fractionation and isotope systematics, in: Stable Isotopes in High Temperature Geologic Processes, H.P.T. J.W. Valley, Jr., J.R. O'Neil, ed., Rev. in Mineral. 16, pp. 227-269, Mineral. Soc. Amer., Chelsea, MI, 1986.

20 S.D. Balsley, A combined stratigraphic, chronologic and petrologic study of an Oligocene post-collapse pyroclastic sequence, southeast San Juan Mountains, Colorado: the Middle Tuff Member of the Treasure Mountain Tuff, Unpublished Ph.D. dissertation, Southern Methodist University, 1994.

21 S.D. Balsley and R.T. Gregory, Oxygen isotope evidence for assimilation of low ^{18}O crust in minor-volume pyroclastic rocks, SE San Juan volcanic field, G.S.A. Abs. Prog. 26(7), A476, 1994.

22 H.P. Taylor, Jr. and S. Epstein, Relationship between $^{18}O/^{16}O$ ratios in coexisting minerals in igneous and metamorphic rocks. Part 2. Applications to petrologic problems, Geol Soc Amer Bull 73, 480-498, 1962.

23 J. Borthwick and R.S. Harmon, A note regarding ClF_3 as an alternative to BrF_5 for oxygen isotope analysis, Geochim. Cosmochim. Acta 46, 1665-1668, 1982.

24 P.W. Lipman, T.A. Steven and H.H. Mehnert, Volcanic history of the San Juan Mountains, Colorado, as indicated by Potassium-Argon dating, Geol. Soc. Amer. Bull. 81, 2329-2352, 1970.

25 P.W. Lipman, M.A. Dungan, L.L. Brown and A. Deino, Recurrent eruption and subsidence at the Platoro caldera complex, southeastern San Juan volcanic field, Colorado: new tales from old tuffs, Geol. Soc. Amer. Bull. 108, 1039-1055, 1996.

26 H.H. Mehnert, P.W. Lipman and T.A. Steven, Age of mineralization at Summitville, Colorado, as indicated by K-Ar dating of alunites, Econ. Geol. 68, 399-401, 1973.

27 T.A. Steven and J.C. Ratte, Geology and ore deposits of the Summitville district, San Juan Mountains, Colorado, U.S. Geol. Survey Prof. Paper 343, 70 p., 1960.

28 M.T. Colucci, M.A. Dungan, D. Lux and P.W. Lipman, Petrologic evolution of the Conejos Formation: intermediate volcanism of the Platoro caldera complex, southeast San Juan volcanic field, Colorado, Geo. Soc. Amer. Abstr. Prog. 19(5), 267, 1987.

29 P.W. Lipman, B.R. Doe, C.E. Hedge and T.A. Steven, Petrologic evolution of the San Juan volcanic field, southwestern Colorado: Pb and Sr isotopic evidence, Geol. Soc. Amer. Bull. 89, 59-82, 1978.

30 V.C. Bennett and D.J. DePaolo, Proterozoic crustal history of the western United States as determined by neodymium isotopic mapping, Geol. Soc. Amer. Bull. 99, 674-685, 1987.

31 H.P. Taylor, Jr., The oxygen isotope geochemistry of igneous rocks, Contrib Mineral Petrol 19, 1-71, 1968.

32 R.L. Christiansen, Yellowstone magmatic evolution: its bearing on understanding large-volume explosive volcanism, in: Explosive Volcanism, F.R. Boyd, ed., pp. 84-95, Nat'l. Acad. Sci., Washington, D.C., 1983.

33 W. Hildreth, A.N. Halliday and R.L. Christiansen, Isotopic and chemical evidence concerning the genesis and contamination of basaltic and rhyolitic magma beneath the Yellowstone Plateau volcanic field, J Petrol 32, 599-624, 1991.

34 H.P. Taylor, Jr., Oxygen and hydrogen isotope evidence for large-scale circulation and interaction between ground waters and igneous intrusions, with particular reference to the San Juan volcanic field, Colorado, in: Geochemical transport and

kinetics, A.W. Hofmann, B.J. Giletti, H. Yoder and R.A. Yund, eds. 634, pp. 299-324, Carnegie Inst., Washington, D.C., 1974.

35 H.P. Taylor, Jr., Water/rock interactions and the origin of H_2O in granitic batholiths, J Geol Soc Lond 133, 509-558, 1977.

36 H.P. Taylor, Jr., Oxygen and hydrogen isotope studies of hydrothermal interactions at submarine and subaerial spreading centers, in: Hydrothermal processes at seafloor spreading centers., P.A. Rona, K. Bostrum, L. Laubier and K.L. Smith, eds. NATO Conf. Ser. Marine Sci. 12, pp. 83-104, Plenum Press, New York, 1983.

37 H.P. Taylor, Jr., Comparison of hydrothermal systems in layered gabbros and granites, and the origin of low-^{18}O magmas, in: Magmatic Processes: Physiochemical Principles., B.O. Mysen, ed. Special Publication 1, pp. 337-357, The Geochemical Society, 1987.

38 I. Friedman, R. Smith and W. Long, Hydration of natural glass and formation of perlite, Geol Soc Amer Bull 77, 323-328, 1966.

39 R.B. Scott, Chemical variations in glass shards and interstitial dust of ignimbrite cooling units, Amer. J. Sci. 270, 166-173, 1971.

40 P.A. Jezek and D.C. Noble, Natural hydration and ion exchange of obsidian: an electron microprobe study, Amer. Mineral. 63, 266-273, 1978.

41 I.S.T. Tsong, C.A. Houser, N.A. Yusef, R.F. Messier, W.B. White and J.W. Michels, Obsidian hydration profiles measured by sputter-induced optical emission, Science 201, 339-341, 1978.

42 T.E. Cerling, F.H. Brown and J.R. Bowman, Low temperature alteration of volcanic glass: hydration, Na, K, ^{18}O, and Ar mobility, Chem. Geol. 52, 281-293, 1985.

43 C.S. Ross and R.L. Smith, Water and other volatiles in volcanic glass, Amer. Mineral. 40, 1071-1089, 1955.

44 C.S. Ross, Volatiles in volcanic glasses and their stability relations, Amer. Mineral. 49, 258-269, 1964.

45 I. Friedman, W. Long and R.L. Smith, Viscosity and water content of rhyolitic glass, J. Geophys. Res. 68, 6523-6535, 1963.

46 G.P. Eaton, R.L. Christiansen, H.M. Iyer, D.R. Mabey, H.R. Blank, Jr., I. Zeitz and M.E. Gettings, Magma beneath Yellowstone National Park, Science 188, 787-796, 1975.

47 R.B. Smith and R.L. Christiansen, Yellowstone Park as a window to the earth's interior, Sci. Amer. 242, 84-95, 1980.

48 R.B. Smith and L.W. Braile, Crustal structure and evolution of an explosive silicic volcanic system at Yellowstone, in: Explosive Volcanism, F.R. Boyd, ed., pp. 96-109, National Academy of Sciences, Washington, D.C., 1983.

49 C.W. Burnham, The importance of volatile components, in: The Evolution of the Igneous Rocks; Fiftieth Anniversary Perspectives., H.S. Yoder, ed., pp. 439-482, Princeton University Press, Princeton, N. J., 1979.

50 C. Merzbacher and D.H. Eggler, A magmatic geohygrometer: application to the Mount St. Helens and other dacitic magmas, Geology 12, 587-590, 1984.

51 S. Newman, S. Epstein and E.M. Stolper, Water, carbon dioxide and hydrogen isotopes in glasses from the ca. 1340 A. D. eruption of the Mono Craters, California: constraints on degassing phenomena and initial volatile content, J. Volcanol. Geotherm. Res. 35, 75-96, 1988.

52 A.T. Anderson, Jr., S. Newman, S.N. Williams, T.H. Druitt, C. Skirius and E. Stolper, H_2O, CO_2, Cl and gas in Plinian and ash-flow Bishop Tuff rhyolite, Geology 17, 221-225, 1989.

53 R.L. Hervig, N. Dunbar, H.R. Westrich and P.R. Kyle, Pre-eruptive water content of rhyolitic magmas as determined by ion microprobe analyses of melt inclusions in phenocrysts, J Volcanol Geotherm Res 36, 293-302, 1989.

54 J.D. Webster and W.A. Duffield, Pre-eruptive concentrations of volatiles and lithophile elements in Taylor Creek Rhyolite: analysis of glass inclusions in quartz phenocrysts, Amer. Mineral. 76, 1628-1645, 1991.

55 M.C. Johnson, A.T. Anderson and M.J. Rutherford, Pre-eruptive volatile contents of magmas, in: Volatiles in magmas, P.H. Ribbe, ed. 30, pp. 281-330, Mineralogical Society of America, Washington, D. C., 1994.

56 D.J. DePaolo, Trace element and isotopic effects of combined wallrock assimilation and fractional crystallization, Earth Planet. Sci. Lett. 53, 189-202, 1981.

57 A. Ewart, A review of the mineralogy and chemistry of Tertiary-Recent dacitic, latitic, rhyolitic and related rocks, in: Trondhjemites, dacites and related rocks., F. Baker, ed., Elsevier, Amsterdam, 1979.

58 D.A. Sawyer, J.R. Budhan, A.M. Sarna-Wojcicki and J.D. Obradovich, New chemical criteria for Quaternary Yellowstone tephra layers in central and western North America, Geol. Soc. Amer. Prog. Abstr. 27(6), A109, 1995.

Table Captions

Table 1. Oxygen isotope and chemical data from the Middle Tuff. Included are the pumice types from which each mineral separate was extracted.

Table 2. Chemical and oxygen isotope data from representative regional ignimbrite units, southeast San Juan volcanic field, Colorado.

Table 3. Age, SiO_2, whole-rock H_2O and quartz $\delta^{18}O$ data of representative units from the Yellowstone volcanic field.

Figure Captions

Figure 1. Location of the Yellowstone and Platoro caldera complexes.

Figure 2. Modal compositions of Middle Tuff andesite through silicic dacite pumice types from the Platoro caldera complex [20].

Figure 3. Plagioclase $\delta^{18}O$ versus augite, biotite and hornblende $\delta^{18}O$ (‰, VSMOW). The field of regional tuffs (n=5) is shown for comparison.

Figure 4. Histogram comparison of plagioclase $\delta^{18}O$ (‰, VSMOW) compositions among Middle Tuff and regional ignimbrites of the Platoro caldera complex. Middle Tuff samples are on average 0.3‰ depleted relative to the larger volume ignimbrites.

Figure 5. Histogram of quartz oxygen isotope ratios (‰, VSMOW) from the Yellowstone volcanic field. [16].

Figure 6. AFC calculations illustrating the effect of magma chamber size on the efficiency of assimilation (initial magma $\delta^{18}O = 7$; contaminant $\delta^{18}O = -11$). "R" is the ratio of cumulates to assimilant. Assuming two spherical magma bodies with volumes of 50 and 500 cubic km, the surface area to volume ratio is approximately two times greater (5 versus 10) for the smaller body. Therefore, the potential for wallrock assimilation is considerably greater for

small volume magmas. Small-volume magmas with lower cumulate-to-assimilant ratios are considerably more sensitive to oxygen isotope modifications than larger bodies.

Figure 7. AFC and water saturation index model curves plotted as a function of fraction of magma crystallized (F). W.S.I. = water saturation index, which is the actual water content the magma divided by the water content of the magma at saturation. Starting magma $\delta^{18}O = 7$ and contaminant = -11. At water saturation, we assume magmas erupt or quench as pressure lowers. This is a consequence of the large volume change of water upon exsolution. Water saturation index curves (0.5, 0.75 and 0.85) are shown for AFC model with $R = 5$ and $\beta = 0.2$ as a function of fraction crystallized. The shaded region represents the approximate range of low-^{18}O Yellowstone rhyolites. Also shown is a histogram of the volume percent crystals (x-axis) of 1650 silicic volcanic rocks examined by Ewart [57] . The peak of the distribution is at a frequency of 0.08. Note that most silicic magmas erupt well before reaching 40% crystallization. Along the water saturation index = 1 line we project up to the $\delta^{18}O$ curve to show hypothetical magmatic values before eruption.

Table 1.
Middle Tuff Oxygen Isotope Data

Sample Number	Pumice Type[1]	Plagioclase δ^{18}O (‰ SMOW)[2]	Augite δ^{18}O (‰ SMOW)	Biotite δ^{18}O (‰ SMOW)	Hbld. δ^{18}O (‰ SMOW)
SB-14	1	6.5			
SB-9	1	6.5	5.6		
SB-10	1	6.3	5.4	5.5	5.5
SB-65	1	6.7 ± 0.1			
SB-114A	1	6.5 ± 0.1			
SB-21	1	6.4			
SB-29	1	6.7			
SB-79	2		5.9	8.2	6.2
SB-78	2	6.7			
SB-17	2	6.8 ± 0.1			
SB-170	2	5.9			
SB-168	2	6.2			
SB-166	2	6.7			
SB-139	3	6.7	5.7	6.1	
SB-95	3	5.6 ± 0.2	6.4	6.1	
SB-96	3	6.5 ± 0.6	6.2	6.3	7.1
MD-74	3	6.1			
SB-26a	af	6.7 ± 0.1			
SB-160	af	6.2 ± 0.2			
SB-173	af	6.4 ± 0.1			
SB-175	af	6.5			
SB-187	af	6.3 ± 0.2			
SB-102	af		6.0	6.1	5.4
SB-9.1	af	6.6			
SB-186	af	6.6			
SB-186a	af	6.3 ± 0.1			
SB-176	af	6.8	6.1	6.6	
SB-188	af	6.4 ± 0.1			
SB-22	v	6.6 ± 0.2			
SB-62	v	6.6 ± 0.2	6.0	7.9	
SB-3	v				
MD-81F	v	6.5			
MD-97	v	6.4 ± 0.2	6.4	4.6	

---

[1] Types 1 through 3: dacite and silicic dacite pumice from flow units. Silicic dacite pumice collected from airfall deposits designated "af." Silicic dacite fiamme collected from vitrophyres designated "v." Andesite pumice designated "a."

[2] Standard deviation calculated from two or more analyses. SMOW = Standard Mean Ocean Water reference standard.

SB-13	a	6.4		5.6	6.4
SB-83	a	6.2 ± 0.3	5.1	6.1	5.7
SB-31	a	5.5 ± 0.1	6.6	6.7	4.9
SB-80	a	6.6 ± 0.1			
SB-101	a	6.8 ± 0.1	6.3	10.9	6.5

Table 2.
Oxygen Isotope Data
Regional Ignimbrites, Platoro Caldera Complex

Sample Number	Unit[a]	SiO_2 (wt.%)[b]	Plagioclase $\delta^{18}O$ (‰ SMOW)[c]	Sanidine $\delta^{18}O$ (‰ SMOW)	Augite $\delta^{18}O$ (‰ SMOW)	Biotite $\delta^{18}O$ (‰ SMOW)
MD-192	Tmp		6.88	7.25	6.21	8.65
MD-167	Tmp	70	6.86 ± .18	6.40		
MD-165	Ttr		6.88	7.28		
MD-43	Ttr		6.98 ± .50			6.43
MD-76	Tto	68	6.82 ± .01			7.17
MD-6	Tto	70				5.61
MD-8A	Ttj	64	6.92 ± .04	7.46	5.96 ± .20	6.43 ± .05
MD-34	Ttj	67	6.70 ± .08		7.47 ± .17	5.48 ± .05
MD-193	Ttj		6.73 ± .11			

---

[a] Map unit designations as follows: Tmp- Masonic Park Tuff; Ttr: Ra Jadero Member; Tto- Ojito Creek Member; Ttj- La Jara Canyon Member.

[b] Whole-rock pumice x-ray fluorescence analysis.

[c] Standard deviation calculated from two or more analyses. SMOW = Standard Mean Ocean Water reference standard.

Table 3.
Yellowstone Rhyolites: Representative Chemical Data*

Caldera Cycle	Caldera-related Ignimbrites	Post-collapse Rhyolites	Age (Ma)	SiO_2 (wt.%)	H_2O (wt.%)	$\delta^{18}O_{qtz}$ (‰ SMOW)
III		*Biscuit Basin Flow*	0.54	72.1	2.8	1.0
		Canyon Flow	0.6	74.7	1.7	1.6
		Tuff of Sulfur Creek	0.6	76.3	2.6	1.5
		Tuff of Uncle Tom's Trail	--	--	--	1.3
	Lava Creek Tuff		0.64[†]	76.1	2.1	6.5
II		*Lookout Butte Dome*	≈1.2	74.7	2.1	5.6
	Mesa Falls Tuff		1.3	75.5	1.44	5.9
I		*Headquarters Flow*	1.8	76.1	0.34	4.0
		Blue Creek Flow	1.8	75.9	0.37	3.8
	Huckleberry Ridge Tuff		2.0	73.0	1.9	7.1

* Compositional data and age determinations for Yellowstone volcanics. SiO_2, H_2O and $\delta^{18}O$ quartz data were averaged for units where there was more than one analysis [16, 33].

[†] [58].

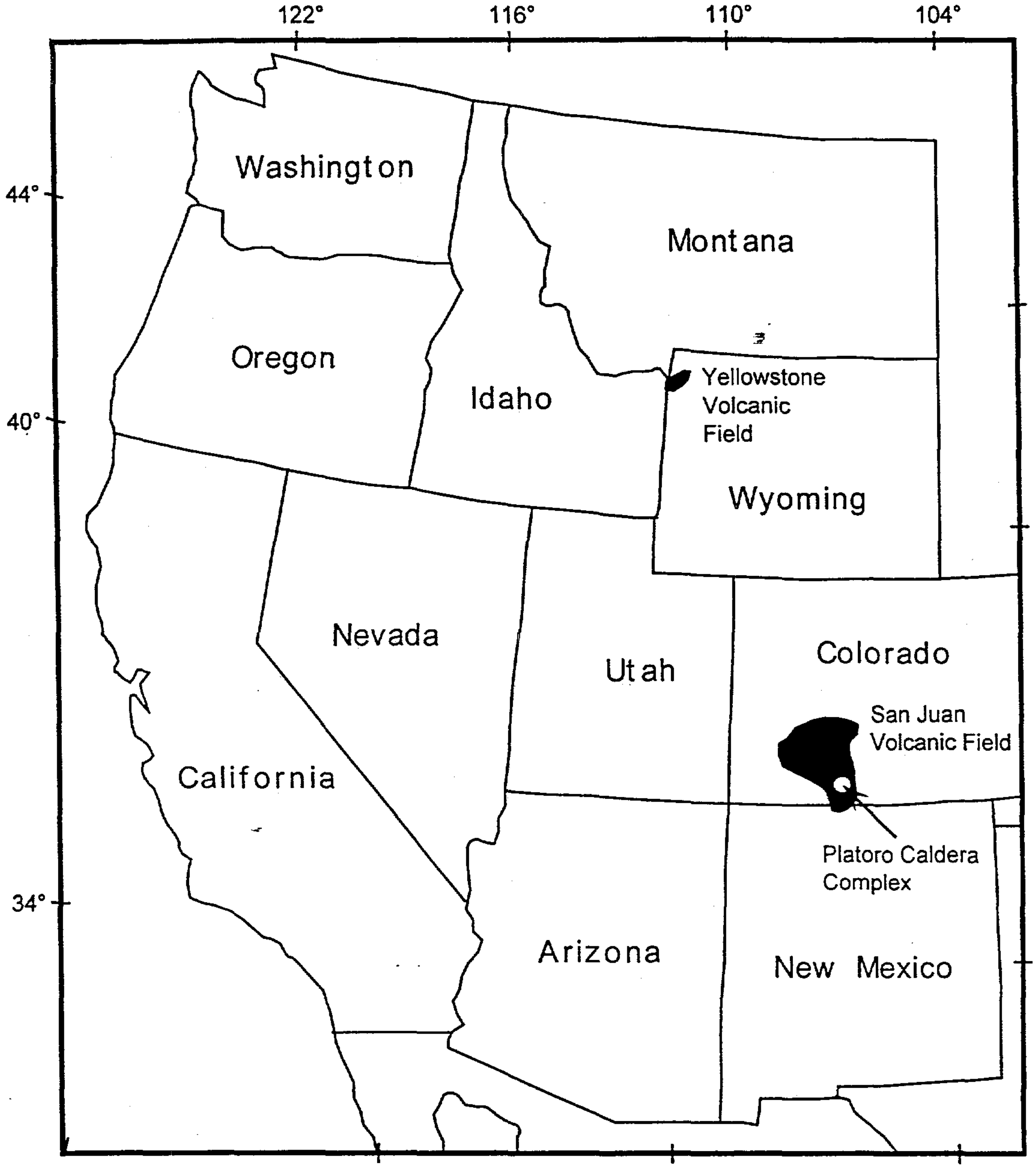
122°
116°
110°
104°
44°
40°
34°
Washington
Montana
Oregon
Idaho
Yellowstone
Volcanic
Field
Wyoming
Nevada
Utah
Colorado
San Juan
Volcanic Field
California
Platoro Caldera
Complex
Arizona
New Mexico

FIGURE 1

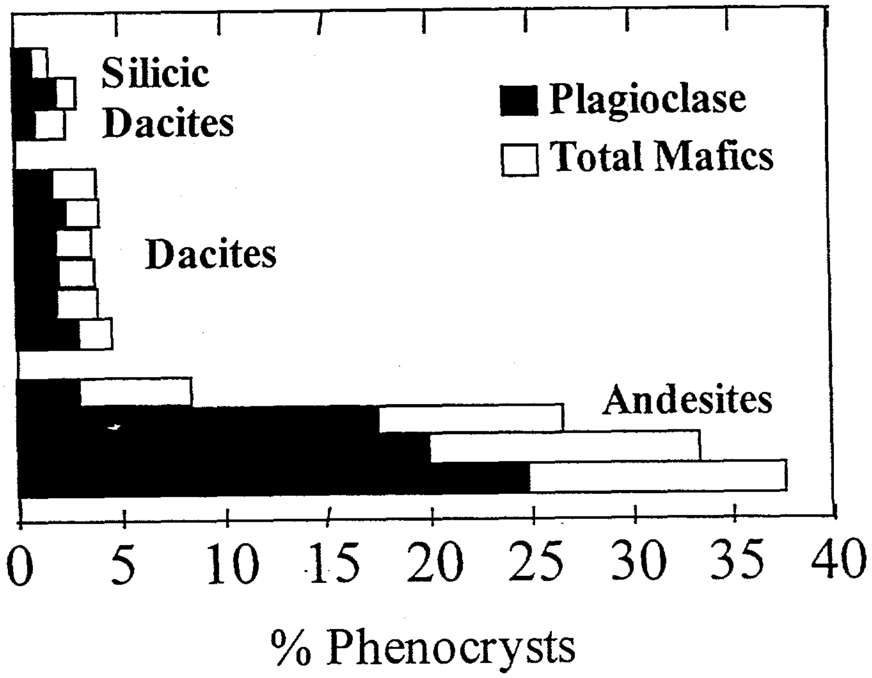
Silicic Dacites
Dacites
Andesites
■ Plagioclase
☐ Total Mafics
0
5
10
15
20
25
30
35
40
% Phenocrysts

FIGURE 2

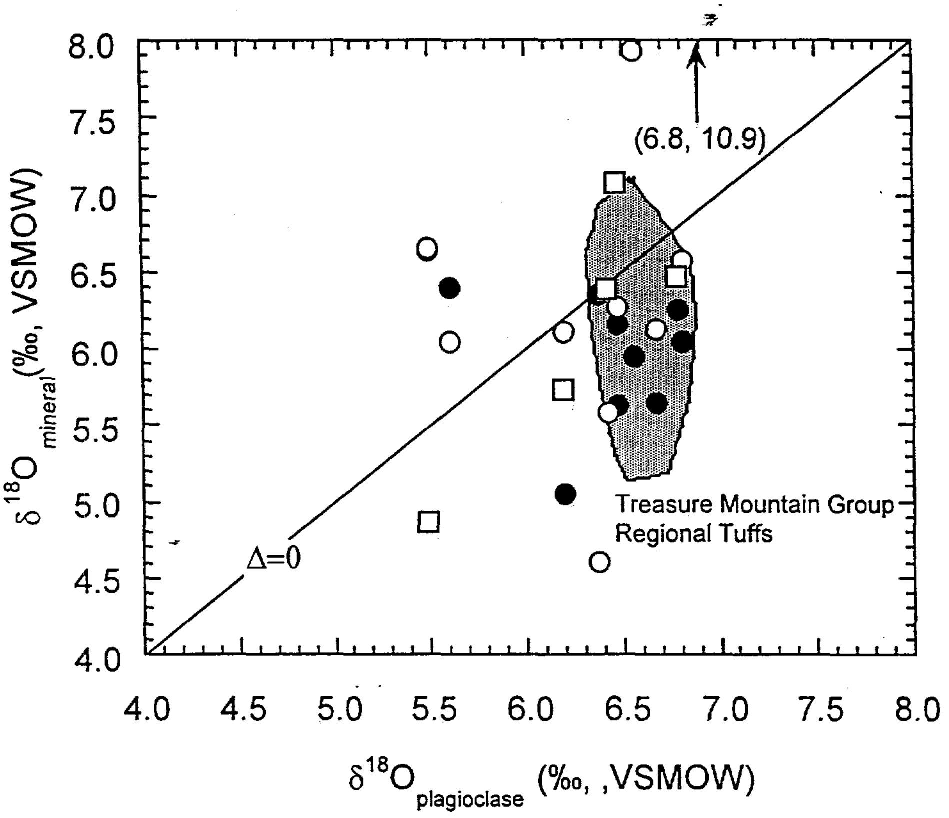
8.0
7.5
7.0
6.5
6.0
5.5
5.0
4.5
4.0
4.0
4.5
5.0
5.5
6.0
6.5
7.0
7.5
8.0
$\delta^{18}O_{mineral}$ (‰, VSMOW)
$\delta^{18}O_{plagioclase}$ (‰, ,VSMOW)
(6.8, 10.9)
Treasure Mountain Group
Regional Tuffs
Δ=0

FIGURE 3

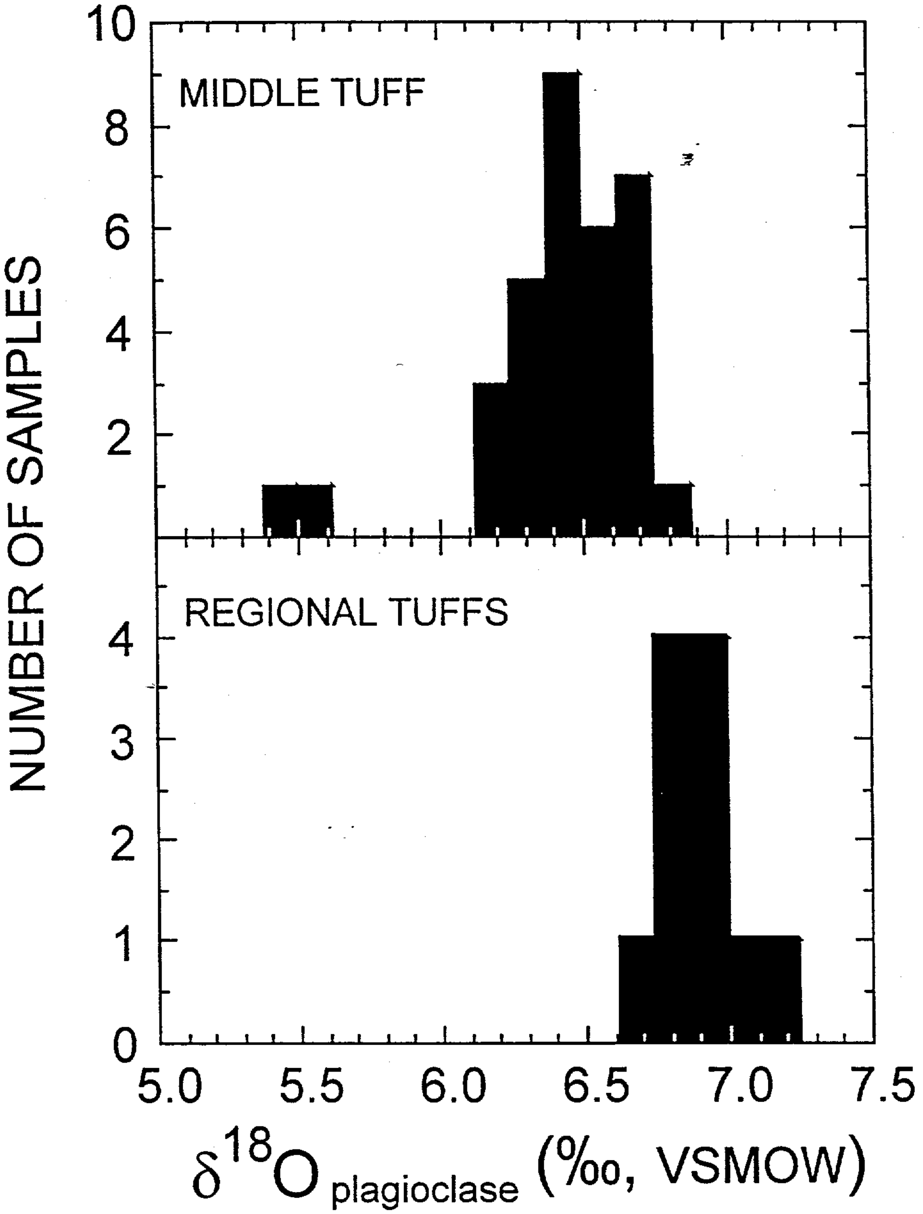
MIDDLE TUFF
REGIONAL TUFFS
NUMBER OF SAMPLES
10
8
6
4
2
4
3
2
1
0
5.0
5.5
6.0
6.5
7.0
7.5
δ18O plagioclase (‰, VSMOW)

FIGURE 4

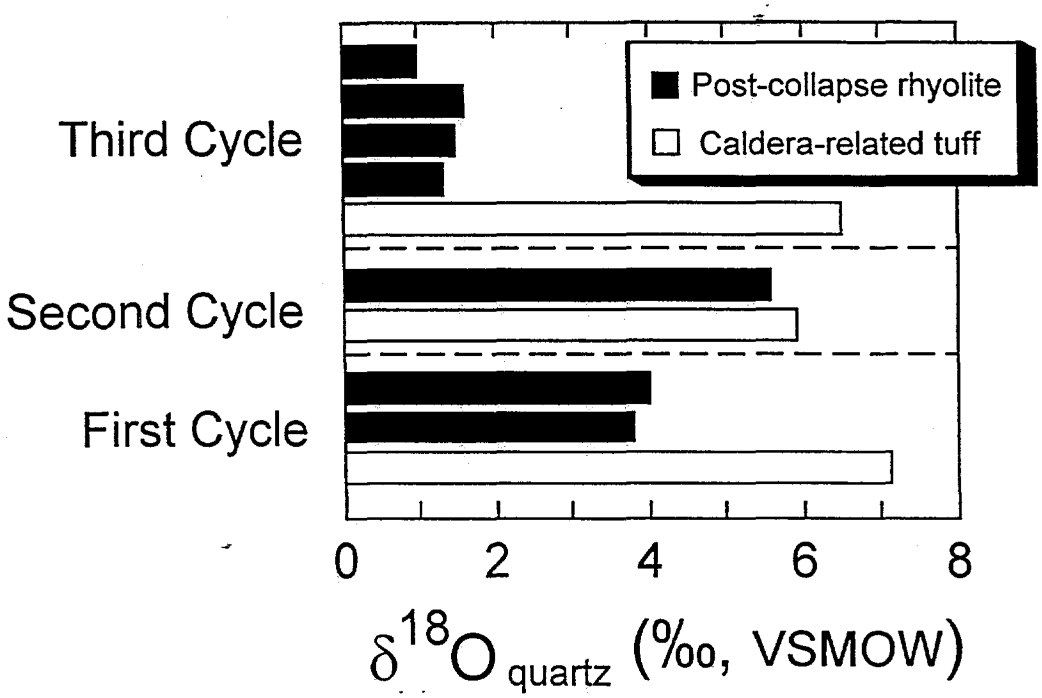
Third Cycle
Second Cycle
First Cycle
■ Post-collapse rhyolite
☐ Caldera-related tuff
0
2
4
6
8
δ18O quartz (‰, VSMOW)

FIGURE 5

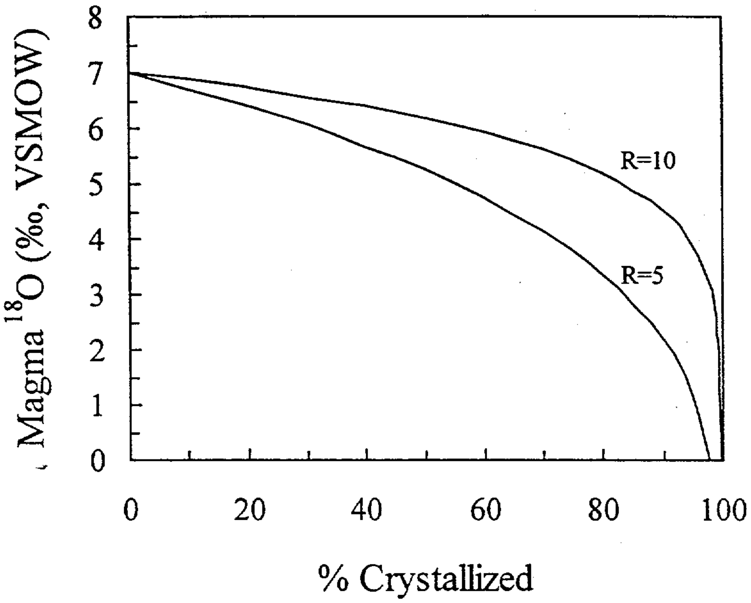
Magma ^{18}O (‰, VSMOW)
0
1
2
3
4
5
6
7
8
0
20
40
60
80
100
% Crystallized
R=10
R=5

FIGURE 6

FIGURE 7